Landslide due to unloading of the hill

Glissement de terrain dû à la décompression d'une colline

R. J. IZBICKI, Lecturer, Technical University of Wrocław, Poland
J. GIERWIELANIEC, Assistant Professor, Technical University of Wrocław, Poland

SYNOPSIS It has become an increasingly frequent practice that technical aspects alone are considered in geotechnic undertaking, while natural conditions are neglected. Such an approach may lead to serious consequences, e.g. to failure during mining operations, to say nothing of a number of adverse economic effects. In this paper, a large landslide of an active nature, which has been contributed by the unloading of the hill, is analyzed. The failure was associated with the removal of a basanite cover from the top of the hill. The total thickness of basanite cover amounted to about 90 m. The volume of the sliding mass has been estimated to be approximately $6x10^4 m^3$ with an approximate weight of $132x10^4$ kN.

INTRODUCTION

The investigations of a basanite quarry and of the immediate vicinity which had been conducted for several years enabled observations of a landslide developing on the western hillside (443.3 m above sea level, Fig.1). Apart from geological field investigations, determinations were carried out for the physical and mechanical features of soil and rocks. Mechanical analysis of the slope stability involved non-conventional methods.
There is no doubt that an appropriate and reliable determination of phenomena associated with landslide requires knowledge of geological conditions. The same knowledge is indispensable when selecting a non-conventional method for stability analysis which are better suited to represent natural reality. It is also essential to have the knowledge of (as well as the ability to predict) the geological and hydrological conditions, when determining the actual values of geotechnical soil-parameters for the considered moment of the process.

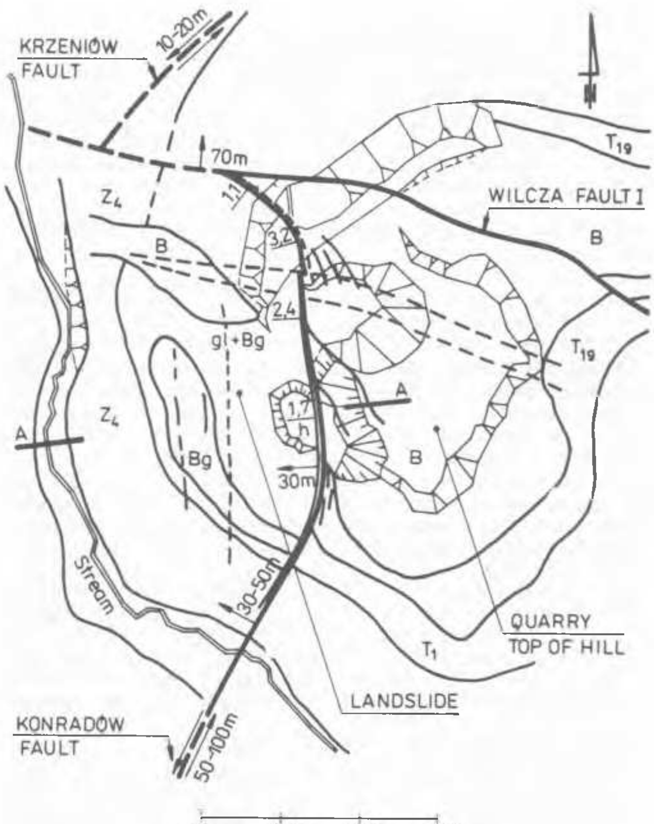

Fig.1 Geological Sketch of the Quarry Area: T_1g - arkose sandstones with basanitic debris, gl+Bg - loam with basanitic debris, Bg - basanitic debris with breccia, B - basanite, T_1 - soft arkose sandstones, Z_4 - sandstones, clay slates and dolomitic limestones, h - taluses of basanites

GEOLOGICAL ASPECTS OF SLIDE

Geology of the area

The region of interest belongs to the Western Sudeten Mountains. It is situated in the south-eastern part of the Kaczawskie Mountains. Its geological structure includes Palaeozoic, Mesozoic and Cainozoic forms.
Palaezoic forms are represented by metamorphic rocks of Ordovician and Silurian systems. They are characterized by the occurrence of grey phyllites (which are predominant there) and diabases (which are predominantly cleaved). The Permian system is not completly developed. It belongs to rotliegendes and Permian limestone. While rotliegendes occurs in the form of con-

glomerates and sandstones with numerous rhyolite inclusions, Permian limestone consists of four cyclothems referred to as Z_1, Z_2, Z_3 and Z_4. The hill contains Z_1 and Z_4. Thus, Z_1 comprises calcium-carboniferous rocks, dolomites, and marls (containing sulphides of copper and other metals). Z_4 begins with a plate dolomite with superimposed bunter sandstone shales, sandstone interbeddings and sandstone.
Mesozoic forms are represented by the Triassic system with bunter sandstone alone (also containing arkoss).
Cainozoic forms include Tertiary and Quaternary systems. Tertiary is represented by basanites alone. They constitute the top, as well as the northern and south-western slopes of the hill. Predominant are black, cohesive basanites having a column-like structure. The southern, eastern and western slopes of the hill are founded on volcanic breccia. The Quaternary system is not complete. The area under study consists of rubble, boulder clay, as well as of blocks of rocks, all of them resting on the Z_4 Permian and Lower Triassic sandstones. Predominant are sandy clays including basanite and volcanic breccia.

Tectonics

The area is characterized by the occurrence of faults of SW and SE direction: Wilcza Fault I and Wilcza Fault II are running parallel to one another to delimit a rift valley. In the vicinity of the hill, the northern section of Wilcza Fault I is lower than its southern section by 70.0 m. The basanites occurring there are highly cracked, brecciated and cleaved. Wilcza Fault II with its throw of fault amplitude of 40 to 100 m accounts for the depression in its southern section.
Konradów Fault (having an almost N-S direction) brings about a movement of Ordovician, rotliegendes and Permian limestone forms along a distance of 50 to 100 m to throw them away within 30 and 50 m. In the W direction the fault surface shows a dip at an angle of 30 to 45 . The western part of the fault (at the point of landslide) consists of basanitic debris in a combination with boulder clay and tectonic clays (formed as a result of trituration of volcanic breccia, Permian sandstone and plate limestone). The eastern section of the fault surface exhibits strongly cleaved basanites. In general, this is a fault zone with a number of cracks and small faults running parallel to one another. Krzeniów Fault (WSW-ENE direction) develops along the bed of an intermittent stream and displaces the alluvium of the Lower Triassic and Permian limestone at a distance between 10 and 20 m.
The major type of tectonic deformations found in this area is rock cracks. Prevailing cracking direction is that of NW-SE and that of NE-SW. They are characterized by a wide range of angles of dip. Cracks developing in the NNW-SSE direction are less frequent.

Water system

The water system in the area under study consists primarily of rain water and underground water discharged from Permian and Lower Triassic sandstones.

CHARACTERISTIC OF LANDSLIDE

It is the Konradów Fault that forms the upper edge of the landslide. In its lower part, the slide rest on a deep valley of a stream (Fig.1). The development of the landslide became evident in 1978 during levelling on the western slope of the hill, when about $4\times10^5\,m^3$ of rock material had been removed. The slide developed in a number of successive stages and is still active. The slip surface were found to develop parallel or perpendicular to the fault planes, in the lithological interface between the Z_4 sandstone and clay slate.

The 1979-1981 survey data show that the edge of the landslide depresses continually (-3.4m). The suspended section of the Konradów Fault was found to have risen by +0.358 m in that period of time. The positive vertical movement of the basanite hill is supposed to be associated with the unloading of the rock mass.

ANALYSIS OF THE SLOPE CRITICAL EQUILIBRIUM

Taking into account the occurrence of determined slip surfaces which appear on the soil mass in the form of fault, cracks and small faults, a non-conventional method was applied to stability analysis (called the generalized limit equilibrium method, GLEM). In this method, the inclinations of the slices may be known in advance or they may be chosen in such a way that a kinematic slip mechanism will develop. The idea of inclined failure planes inside the failed mass was made use of by Karal (1977). The GLEM belongs to the class of upper bound solutions in the theory of plasticity (cf. Kisiel et al., 1981). Hence, for the critical equilibrium and the associated flow law, the upper bound of the extermination parameter (F = factor of safety, P = external load, etc.) can be obtained

(i) from total work balance (energy approach, Karal, 1977),
(ii) or by making use of the equilibrium conditions for the field of forces associated with the assumed kinematically admissible failure mechanism (equilibrium approach).

Both approaches are equivalent. In this paper, we apply the equilibrium approach.
The internal forces acting on the ith slice are shown in Fig.2. The co-ordinates of the points where the forces are acting, are denotes as x_{1i}, y_{1i} etc. For brevity, we write $\sin\alpha_{1i} = S_{1i}$, $\cos\alpha_{1i} = C_{1i}$, etc. The co-ordinates of the centre of gravity S are x_{Si}, y_{Si}.
The three equations of equilibrium for the slice may be written in a matrix form

$$\begin{bmatrix} 0 \\ -W_i \\ 0 \end{bmatrix} + \begin{bmatrix} \Sigma P_{xj} \\ \Sigma P_{yj} \\ \Sigma(P_{xj}y'_j - P_{yj}x'_j + M_j) \end{bmatrix} = \qquad (1)$$

$$= \begin{bmatrix} -C_{1i} & S_{1i} & 0 \\ -S_{1i} & -C_{1i} & 0 \\ S_{1i}x'_{1i} - C_{1i}y'_{1i} & C_{1i}x'_{1i} + S_{1i}y'_{1i} & 0 \end{bmatrix} \begin{bmatrix} N_{1i} \\ kT_{1i} \\ 0 \end{bmatrix} +$$

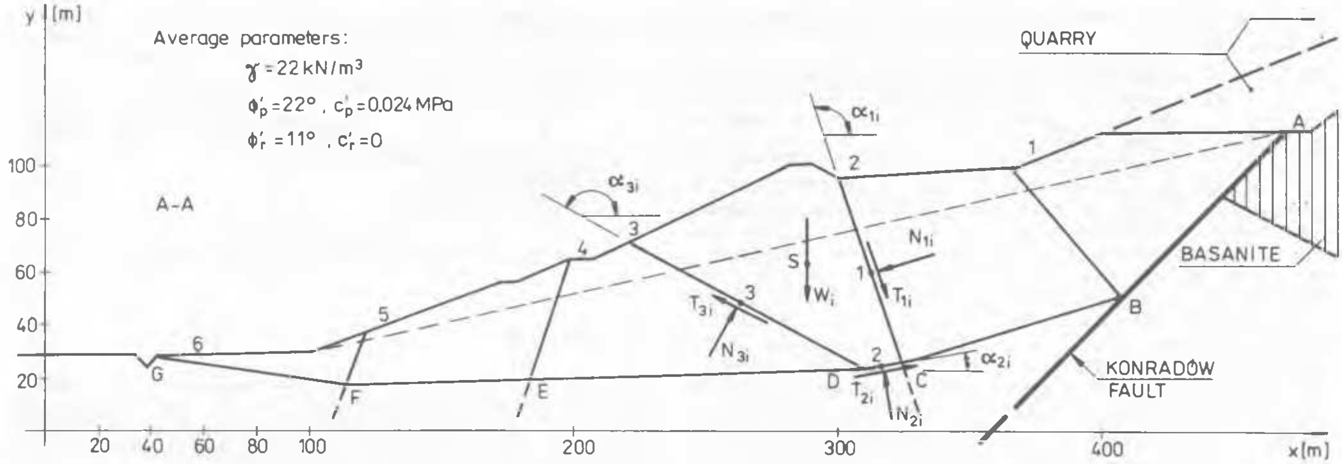

Fig.2 Failure Mechanism for Critical State

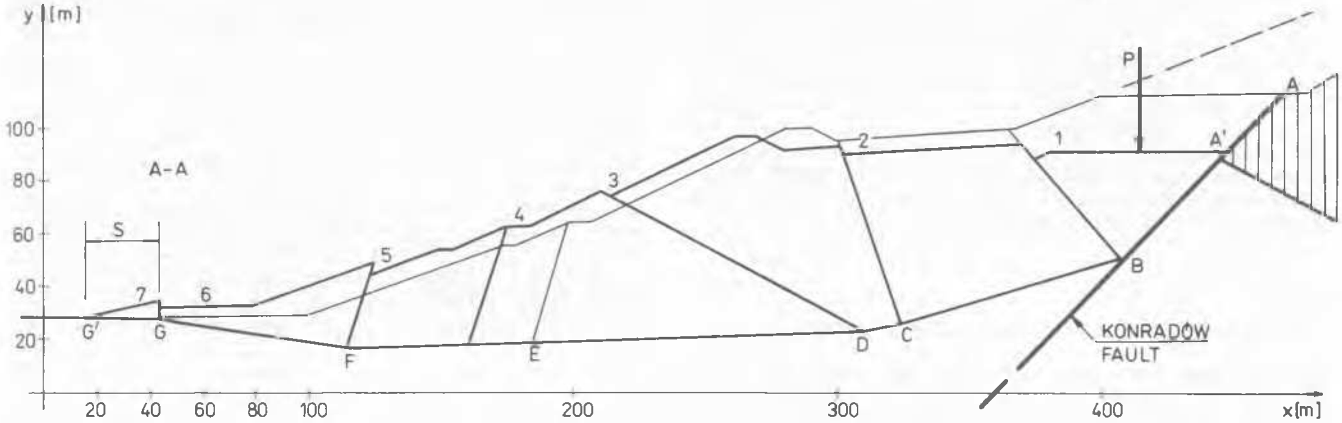

Fig.3 Failure Mechanism for Post-Critical State

$$
+\begin{bmatrix} -C_{2i} & S_{2i} & 0 \\ -S_{2i} & C_{2i} & 0 \\ S_{2i}x'_{2i}-C_{2i}y'_{2i} & C_{2i}x'_{2i}+S_{2i}y'_{2i} & 0 \end{bmatrix} \begin{bmatrix} N_{2i} \\ kT_{2i} \\ 0 \end{bmatrix} +
$$

$$
+\begin{bmatrix} C_{3i} & S_{3i} & 0 \\ -S_{3i} & C_{3i} & 0 \\ S_{3i}x'_{3i}+C_{3i}y'_{3i} & -C_{3i}x'_{3i}+S_{3i}y'_{3i} & 0 \end{bmatrix} \begin{bmatrix} N_{3i} \\ kT_{3i} \\ 0 \end{bmatrix}
$$

or as

$$
W_i + P_i = H_{1i}Q_{1i} + H_{2i}Q_{2i} + H_{3i}Q_{3i} , \qquad (2)
$$

where factor $k=\pm 1$ defines the kinematically admissible direction of the shear forces, Σ denotes summation over all of the external loads P_j and moments M_j on the slice and $x'_{1i}=x_{1i}-x_{Si}$, $y'_{1i}=y_{1i}-y_{Si}$, etc.

For all slices, the equations of equilibrium can take a matrix form

$$
\underline{W} + \underline{P} = \underline{H}\underline{Q} \quad , \qquad (3)
$$

where $\underline{W}$ is body forces vector, $\underline{P}$ is external load vector, $\underline{Q}$ is a vector of internal interactions on the surfaces bounding the slice, and $\underline{H}$ is coefficient matrix.

Assume that the factor of safety on the internal shear planes and on the slip surface are identical. Thus, by virtue of the Coulomb failure condition, we may write for all of the internal forces

$$
T = \frac{1}{F_k}\left[(N-U)\tan\phi' + c'l\right] \quad , \qquad (4)
$$

where U is force due to pore water pressure, F_k indicates the upper bound to the factor of safety, and l denotes the length of shear plane.

Of the set of Eqs.3, considering Egs.4, the equations describing the vertical and horizontal equilibrium are sufficient to determine the upper bound of the factor of safety, as well as the values of internal forces, by applying a procedure of trial and error. The solution for the last slice n requires that the condition $Q_{2n+1,n}=0$ be fulfilled. The equations of moments can be used for determining the line of thrust of forces acting on the internal shear planes (cf. Sarma, 1979).

The GLEM can also be employed in the case of non-associated flow law to the estimation of the kinematical value (not upper bound) of the factor of safety F_{kn}. Then, the average parameters $\tan\phi'$ and c' for failure surfaces should be substituted by

$$
\tan\phi'_s = \frac{\cos\psi\sin\phi'}{1-\sin\psi\sin\phi'} \quad \text{and} \quad c'_s = \frac{c'\cos\psi\cos\phi'}{1-\sin\psi\sin\phi'} \qquad (5)
$$

respectively, where ψ is angle of dilatancy (cf. Davis, 1968).

It is not reasonable to adopt the value of F_k = 1.25 (calculated for peak strength parameters ϕ'_p and c'_p for soil mass, and residual parameters ϕ'_r and c'_r along fault AB, Fig.2), because sliding is a progressive process associated with the unloading of the hill, the reactivation of movements along determined slip surfaces, and the drop of strength to the residual value. In fact, repeating calculations for the residual strength along the cracks and small faults, we obtain an acceptable value of the factor of safety, which is now 0.96. It has been assumed that pore pressure is acting on the slip surface and that the faults are filled with water. This example is a clear indication that the value of the safety factor is influenced by the shear strength on the internal shear surfaces.

It is worth noting that if the non-associated flow law and an incompressibility (ψ=0) are dealt with, the GLEM yields, respectively, the following values of the kinematic estimate, F_{kn} =1.21 and 0.94 (both approach the previously determined values of the upper bound). This result is not surprising in the case of critical equilibrium (cf. Zienkiewicz et al., 1975). Major differences between associated and non-associated flow law were found to occur in the field of deformations in general, and advanced plastic deformations in particular.

ESTIMATION OF POST-FAILURE SLOPE MOVEMENTS

Now estimate how far the sliding mass will travel in the case of a quasi-static motion. Assume that during motion, the mass of slices 1, 2 and 5 decreases and the mass of slices 3, 4, 6 and 7 (forced on the surface of base) increases (Fig.3). Also assume that if the state of advanced plastic deformations occurs, then the non-associated flow law with ψ=0 is valid. The incremental problem can be solved for small variations in geometry.

If a slope is initially in the critical state there may occur an infinitesimal motion along slip surface, when external force P=0 (the value of this force may be interpreted as the slope load capacity margin). It is assumed that, once the critical equilibrium has been exceeded, even at an infinitely small displacements (as compared to their final value), the strength along slip surface immediately drops to residual. To maintain a static equilibrium it is necessary to employ a given force P, of a sense opposite to that shown in Fig.3. The value of this force may be determined from the equilibrium conditions (Eqs.3) for F_{kn}=1. During quasi-static motion associated with the forcing-through of slices 4, 5, 6 and 7 with increasing mass, force P (directed upward) decreases gradually to reach zero at a given displacement value, and from those continues to increase. Thus the value of force P may be plotted by a static curve $L_1M_2L_2L_4$ (Fig.4).

In the case of a quasi-static motion, point L_2 is identical with the point at which the position of a new equilibrium is achieved, and for which the travel distance S_{max} = 50 m.

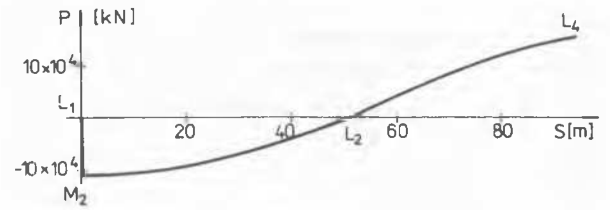

Fig.4 Static Equilibrium Curve

CONCLUSIONS

An appropriate and reliable analysis of landslides requires knowledge of the geological and hydrological conditions. This knowledge makes it possible to select a non-conventional method of stability analysis as well as to determine the actual values of soil strength parameters for the considered moment of the process.

Observations, as well as the mechanical analysis presented here, concern one of the many landslides that originate and develop contemporarily. However, the considerations and methods involved in this study may also be of utility in solving other failure problems.

The methods presented make use of the kinematics of sliding elements. It is obvious that there is still scope for the development of both limit analysis and limit equilibrium methods of stability analysis, in which different procedures may serve different purposes.

REFERENCES

Davis, E.H. (1968). Theories of plasticity and the failure of soil masses. Soil mechanics, selected topics. ed. I.K. Lee, 341-380, Butterworths, London.

Karal, K. (1977). Energy method for soil stability analyses. ASCE J.Geot.Eng.Div., 103, GT5, 431-445.

Kisiel, I., Izbicki, R.J., Skoczylas, K. and Stilger-Szydło, E. (1981). Statical and kinematical approach to slope stability. Proc. 10th ICSMFE, 3, 453-456, Stockholm.

Sarma, S.K. (1979). Stability analysis of embankments and slopes. ASCE J.Geot.Eng. Div., 105, GT12, 1511-1524.

Zienkiewicz, O.C., Humphenson, C. and Lewis, R.W. (1975). Associated and non-associated viscoplasticity and plasticity in soil mechanics. Geotechnique, 25, 671-691.